

# Molecular Theory of Solvent Effect on Keto–Enol Tautomers of Formamide in Aprotic Solvents: RISM-SCF Approach

Tateki Ishida,<sup>†</sup> Fumio Hirata,<sup>‡</sup> Hirofumi Sato,<sup>‡</sup> and Shigeki Kato<sup>\*,†</sup>

Department of Chemistry, Graduate School of Science, Kyoto University, Kitashirakawa, Sakyo-ku, Kyoto 606, Japan, and Institute for Molecular Science, Myodaiji, Okazaki, Aichi 444, Japan

Received: September 26, 1997; In Final Form: January 12, 1998

The reference interaction site model self-consistent-field (RISM-SCF) method is applied to study the solvent effect on the keto–enol tautomers of formamide in aprotic solvents. Six aprotic solvents—carbon tetrachloride (CCl<sub>4</sub>), carbon disulfide (CS<sub>2</sub>), dimethyl ether (DME), tetrahydrofuran (THF), acetonitrile (CH<sub>3</sub>CN), and dimethyl sulfoxide (DMSO)—are examined. We present detailed analyses of the solvent effects on solvation free energies, solvation structures, and solute electronic structures from a microscopic point of view. Good correlation between the calculated depth of the first minimum in the first solvation shell and the empirical solvent parameters representing solute–solvent hydrogen bonding is found, which provides a microscopic interpretation of the parameters. The solvation free energy does not increase monotonically with an increase of solvent polarity, and a remarkable irregularity is seen for acetonitrile.

## I. Introduction

Solvent effects on chemical equilibria and reactions have long been one of the important subjects in physical organic chemistry. Several empirical relations have been proposed to characterize the properties of various protic and aprotic solvents.<sup>1</sup> Among them, the solvent parameters that Taft and co-workers<sup>2</sup> determined taking solute–solvent hydrogen bonding and solvent polarity into account have been applied to rationalize experimentally observed solvent effects. Although these parameters have been qualitatively related to the physical properties of solvent molecules such as hydrogen bonding and solvent polarities in their studies, it seems still far from satisfactory to interpret them on the basis of microscopic information of the solute–solvent interaction and solvation free energy. In particular, the theoretical interpretation based on statistical mechanical treatments of solute–solvent systems is virtually nonexistent to our knowledge. In this respect, it would be worthwhile to carry out theoretical studies on the solvent effects for various protic and aprotic solvents from a unified microscopic point of view.

There has been remarkable progress in the electronic structure theories of solute molecules in solution in the last two decades. Various versions of self-consistent reaction field (SCRF) methods have been advanced<sup>3</sup> to utilize them in interpreting the effects of polar solvents on chemical phenomena. However, many of these methods<sup>4</sup> employ the dielectric continuum model for solvent, characterized by the dielectric constants, and are unable to describe the local solute–solvent interaction such as hydrogen bonding.

Statistical mechanics of liquids has been developed by the approach with the integral equations. The reference interaction site model (RISM) by Chandler and Andersen<sup>5</sup> takes the geometric aspect of molecules into account with the site–site representation for intra- and intermolecular interactions. The extended RISM (XRISM) theory<sup>6–8</sup> has been further devised

to include the Coulombic interaction between molecules by setting partial charges on each atomic site.

Recently, the RISM self-consistent-field (RISM-SCF) method<sup>9–11</sup> has been developed by combining the electronic structure calculations of solute molecules with the RISM theory for solvents and applying it to various problems in solution chemistry.<sup>12–14</sup> This method describes the solute–solvent interaction as the sum of site–site interactions between the constituent atoms in solute and solvent molecules and thus has an advantage in providing a microscopic view of solute–solvent interaction. It is noted that the RISM-SCF method has been applied so far only to the aqueous solutions.<sup>12–14</sup>

Many examples of the solvent effects on chemical equilibria and reactions have been observed. Among them, the solvent effect on the keto–enol tautomerism has been extensively studied.<sup>15,16</sup> Experimentally, it is known that the keto–enol equilibrium constants change depending on the solvent polarity in solution.<sup>17–20</sup> Theoretical studies of the specific systems such as 2-pyridone<sup>1,21</sup> and formamide<sup>1,21,22</sup> have been reported, but in most of them, the solvent was treated as a dielectric continuum and little information was obtained on the structure of solvents around the solute. In these studies, the solvation free energy has been interpreted in relation to the dielectric constants, which are macroscopic properties of solvents and could not be treated from the viewpoint of a microscopic picture.

In this article, we present a theoretical study on the keto–enol tautomerism of formamide in a series of aprotic solvents. We adopted six aprotic solvents including carbon tetrachloride (CCl<sub>4</sub>) and carbon disulfide (CS<sub>2</sub>) as nonpolar ones and dimethyl ether (DME), tetrahydrofuran (THF), acetonitrile (CH<sub>3</sub>CN), and dimethyl sulfoxide (DMSO) as polar ones. We carried out RISM-SCF calculations to obtain the geometries and solvation free energies of the keto and enol tautomers of formamide in these aprotic solvents. In the following section, the details of the calculations are presented. In section III, we present the results of calculations, and the origin of the energy difference between the keto and enol tautomers is discussed by relating the solvation free energy to the characteristics of solvent

<sup>†</sup> Kyoto University.

<sup>‡</sup> Institute for Molecular Science.

**TABLE 1: Parameters for Aprotic Solvents and Solute**

solvent <sup>a</sup>	site	q	$\sigma/\text{\AA}$	$\epsilon/\text{kcal mol}^{-1}$
CCl <sub>4</sub>	C	-0.1616	3.2	0.10
	Cl	0.0404	3.4	0.26
CS <sub>2</sub>	C	-0.308	3.2	0.101
	S	0.154	3.52	0.395
DME	O	-0.50	3.0676	0.179
	CH <sub>3</sub>	0.25	3.8609	0.181
THF	O	-0.50	3.000	0.170
	CH <sub>2</sub> <sup><math>\alpha</math></sup>	0.25	3.800	0.118
	CH <sub>2</sub> <sup><math>\beta</math></sup>	0.00	3.905	0.118
CH <sub>3</sub> CN	CH <sub>3</sub>	0.15	3.775	0.206
	C	0.28	3.650	0.150
	N	-0.43	3.200	0.169
DMSO	O	-0.459	2.80	0.0715
	S	0.139	3.40	0.238
	CH <sub>3</sub>	0.160	3.80	0.293
solute	site	$\sigma/\text{\AA}$	$\epsilon/\text{kcal mol}^{-1}$	
	N <sup>b</sup>	3.25	0.170	
	C <sup>b</sup>	3.75	0.105	
	O <sup>b</sup>	2.96	0.210	
	H <sup>c</sup>	1.78	0.02	

<sup>a</sup> Data from refs 23, 24 for CCl<sub>4</sub>, ref 25 for CS<sub>2</sub>, ref 26 for DME, ref 27 for THF, ref 28 for CH<sub>3</sub>CN, ref 29 for DMSO. <sup>b</sup> Reference 30. <sup>c</sup> Reference 31.

molecules. We further give a microscopic interpretation of Taft's solvent parameters on the basis of the present calculations. The conclusion is given in section IV.

## II. Method

**2.1. Calculation of the Total Correlation Functions of Pure Aprotic Solvents.** In applying the XRISM theory to the solute-solvent systems, it is necessary to solve the RISM Ornstein-Zernike equations:

$$h^v = \omega^v * c^{vv} * \omega^v + \rho \omega^v * c^{vv} * h^{vv} \quad (1)$$

$$h^{uv} = \omega^u * c^{uv} * \omega^v + \rho \omega^u * c^{uv} * h^{vv} \quad (2)$$

where the asterisk denotes the spatial convolution integral,  $h$  and  $c$  stand for the site-site intermolecular pair correlation functions and the direct correlation functions, respectively, and  $\rho$  is the number density of solvent. The indices  $u$  and  $v$  denote the solute and solvent, respectively.  $\omega$  is the intramolecular correlation function that defines the molecular geometry. As the total correlation function,  $h^{vv}$ , for solvent in eq 2, the solutions of eq 1 for pure solvents are used.

The total correlation functions of pure aprotic solvents were obtained by solving eq 1 with the hypernetted chain (HNC) approximation. The geometric parameters, the partial charges on the sites, and the parameters of the 6-12 type potential functions of aprotic solvents were used in the computer simulations.<sup>23-29</sup> All the parameters employed in the present calculations are summarized in Table 1. The Lennard-Jones parameters of solute atoms<sup>30,31</sup> are also included in Table 1.

**2.2. RISM-SCF Calculation.** The details of the RISM-SCF method have been presented in previous papers.<sup>9-11</sup> In determining partial charges on the solute sites, we generated grid points based on the Voronoi polyhedrons<sup>32</sup> and applied the least-squares fitting procedure to the electrostatic potential coming from the solute charge distribution. All the ab initio calculations were performed at the restricted Hartree-Fock (RHF) level by using the double-zeta plus polarization (DZP) basis set.<sup>33</sup> The geometry of the solute molecule was optimized using the analytical energy gradient technique<sup>11</sup> in each solvent studied.

The solvation free energies were calculated with the equation for HNC closure:<sup>34,35</sup>

$$\Delta F_{\text{HNC}} = \frac{\rho}{2\beta} \sum_{\alpha \in u} \sum_{\gamma \in v} \int_0^\infty 4\pi r^2 dr (h_{\alpha\gamma}^2 - 2c_{\alpha\gamma} - h_{\alpha\gamma}c_{\alpha\gamma}) \quad (3)$$

and the total free energy was defined by

$$E_{\text{total}} = E^{\text{sol}}(\text{solute}) + \Delta F_{\text{HNC}} \quad (4)$$

where  $E^{\text{sol}}(\text{solute})$  represents the electronic energy of the solute in solution. In solution, the solute electronic structure changes from that in the gas phase due to the solute-solvent interaction. The energy change associated with the relaxation in the geometry and the electronic structure of the solute is defined as the following:

$$\Delta E_{\text{re}} = E^{\text{sol}}(\text{solute}) - E^{\text{gas}}(\text{solute}) \quad (5)$$

where  $E^{\text{gas}}(\text{solute})$  is the solute energy in the gas phase.

## III. Results and Discussion

**3.1. Solvation Structure.** (a) *Pure Solvent Radial Distribution Function.* We carried out RISM calculations to obtain the radial distribution functions (rdf's) and the total correlation functions, for six aprotic solvents. We used the potential parameters listed in Table 1. The geometric parameters were taken from the literature for all the solvents.<sup>23-29,36</sup> The temperature was set to be 295.15 K for CCl<sub>4</sub> and 298.15 K for other solvents except DME, respectively, and that of DME was 248.35 K. Although the RISM calculations have been reported previously for CCl<sub>4</sub> and CS<sub>2</sub>, the partial charges on the sites were not taken into account in these calculations.<sup>23</sup> Therefore the results of the present calculations are different from those in the previous ones.

Since the present calculations of solvents are for use in the calculations for solutions, we only discuss here the results for THF and DMSO. In Figure 1, the calculated rdf's for pure THF and DMSO are shown and are compared with the computer simulation results for pure THF<sup>27</sup> and DMSO.<sup>29</sup> For THF, the positions and heights of the first and second peaks are in qualitative accord with those obtained by the computer simulation. The rdf for DMSO is rather complicated, as seen in Figure 1b, but the positions and heights of three peaks and the whole profile are similar to those by the computer simulation. Also in both cases, the long-range behavior that appears in the simulation results is reproduced.

(b) *Radial Distribution Functions of Solvent around Solute.* Some of the rdf's between the solute hydrogen atoms, H(4) and H(5) in Figure 2, and solvent atoms are shown in Figure 3a-c. The rdf's in polar aprotic solvents show distinct peaks representing the first and second solvation shells. The height of the first peak is greater than that of the second peak. In solutions of nonpolar aprotic solvents, however, the first peak does not appear clearly and the whole profiles of the rdf's are structureless. In determining the solvation structure, the Coulombic interactions between the solute and the solvents in the neighborhood of the first peak are very important. Especially, the hydrogen atoms with positive partial charges attractively interact with the solvent atoms with negative partial charges and repulsively with the solvent atoms positively charged. Since, as seen in Table 2, H(4) and H(5) of formamide have modest positive charges, the interactions with the nitrogen of acetonitrile and the oxygen of DMSO, which have large negative charges,

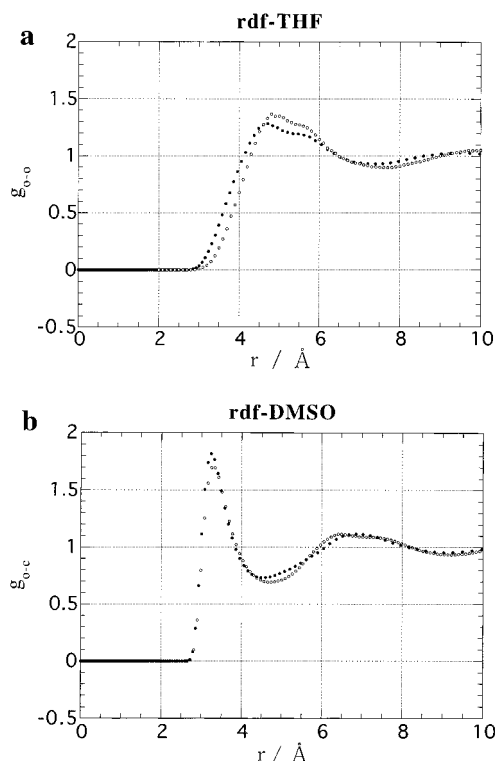


**Figure 1.** (a) O–O radial distribution functions for pure THF. Circles indicate computer simulation results (ref 27). (b) S–O radial distribution functions for pure DMSO. Circles indicate computer simulation results (ref 29).

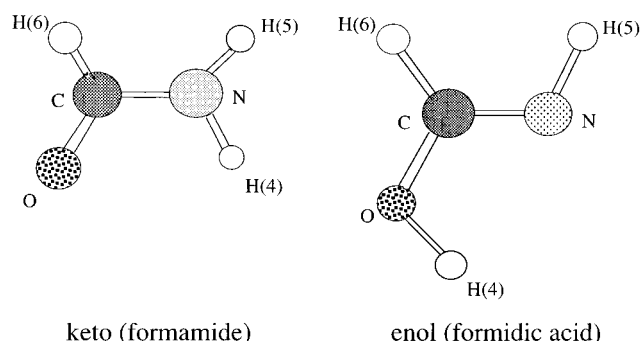


**Figure 2.** Molecular form and site assignment of keto–enol tautomers of formamide.

are attractive due to the Coulombic interaction. These attractive forces produce distinct peaks in the rdf's. Since the chlorine site of  $\text{CCl}_4$  has a small positive charge, the structureless behavior in the rdf's in  $\text{CCl}_4$  solution is caused by the repulsive interaction between positive charges on solute and solvent sites, and this behavior shows that the tendency of forming a solute–solvent hydrogen bond is low.

**3.2. Solvation Energy.** (a) *Comparison of Solvations for Keto and Enol Tautomers.* In Table 3, the optimized geometries of formamide and its tautomer in solutions are shown. In nonpolar aprotic solvents, the structures of both tautomers are very close to the gas phase ones due to weak solute–solvent interactions. In polar aprotic solvents, the  $\text{C}=\text{O}$  distance in formamide is stretched while the  $\text{C}-\text{N}$  bond is shortened. This structural change increases the solute dipole moment and results in a stronger solute–solvent interaction.

In the enol form (formic acid), the intramolecular hydrogen bonding between the nitrogen and hydroxyl hydrogen atom is formed in the gas phase. Its strength seems to be weak, but it affects the distance between the nitrogen and hydrogen. As

seen in Table 3, the  $\text{N}\cdots\text{H}$  distance does not change compared with that in the gas phase in the nonpolar solvents. However, the distance becomes longer in polar solvents than in the gas phase by about 0.05 Å. This is because the intramolecular hydrogen bond is weakened because of the formation of solute–solvent hydrogen bonding. The  $\text{O}-\text{H}$  bond and the  $\text{OCN}$  bending angle are slightly increased in polar solvents, which enhance the solute dipole moment.

The differences in the total free energies between the keto and enol tautomers at the optimized geometries, denoted by  $\Delta G$ , are shown in Table 4. For the solutions of nonpolar solvents, the energy differences between the keto and enol tautomers are almost the same as that in the gas phase. This is because the solvation free energies as well as the solute electronic reorganization energies are very small, since the electrostatic potentials acting on the solute sites are very small in these solvents.

On the other hand, in the solutions of polar aprotic solvents,  $\Delta G$  is larger than that in the gas phase. As seen in Table 4, the differences in the solvation free energies are larger than those in the solute reorganization energies in all solutions. Therefore it is considered that  $\Delta G$  is dominated by the solvation free energy differences. For the keto–enol equilibria, the keto tautomer is stabilized in comparison with the enol one, which is consistent with the larger dipole moment of the keto tautomer than the enol one. This is in qualitative accord with the experimental findings on similar tautomeric systems.<sup>16,18</sup>

(b) *Solvation Free Energy Analyses.* In Table 4, the solvation free energies of the keto and enol form of formamide in aprotic solvents are shown. In nonpolar aprotic solvents, the solvation free energies are of positive values. These are consistent with the tendency that the solubilities of polar solutes in nonpolar solvents are very low. In polar aprotic solvents, the magnitude of the solvation free energy does not increase monotonically as the solvent polarities increase. Especially, as seen in Table 4, the irregularity of the solvation free energy in acetonitrile is remarkable for both the keto and enol forms. This irregularity in acetonitrile cannot be explained by the conventional dielectric continuum model, because the magnitude of the solvation free energy increases with the increase of the dielectric constant of solvents<sup>37</sup> (see Table 4).

We further estimated the solvation free energies with the assumption of Gaussian fluctuations (GF) by Chandler et al.<sup>33</sup> Although the solvation free energies by the GF approximation are systematically larger than the HNC results in Table 4, the qualitative tendency is the same and the irregularity is also observed for acetonitrile. Therefore we will use the results of the HNC equation for further analyses.

To clarify the origin of irregular order of solvation energy, we carried out decomposition analyses of solvation free energy. Since the expression for solvation free energy, eq 3, is “formally” a sum of the solute–solvent site–site interactions, we define the contribution of the solute atom, for example, atom  $\alpha$ , to the solvation free energy by

$$\Delta F_{\text{HNC}}^{\alpha} = \frac{\rho}{2\beta} \sum_{\gamma \in v} 4\pi r^2 dr (h_{\alpha\gamma}^2 - 2c_{\alpha\gamma} - h_{\alpha\gamma}c_{\alpha\gamma}) \quad (6)$$

It should be noted that  $\Delta F_{\text{HNC}}^{\alpha}$  is not the same as the solvation free energy of atom  $\alpha$  when the atom is placed in the solvent by itself. The results for  $\Delta F_{\text{HNC}}^{\alpha}$  are shown in Table 5. In the keto form, the stabilization energies assigned to the solute hydrogen sites, H(4) and H(5), are the largest. Also the solvation free energies for the solute carbon and oxygen sites have negative values though the contributions are smaller than

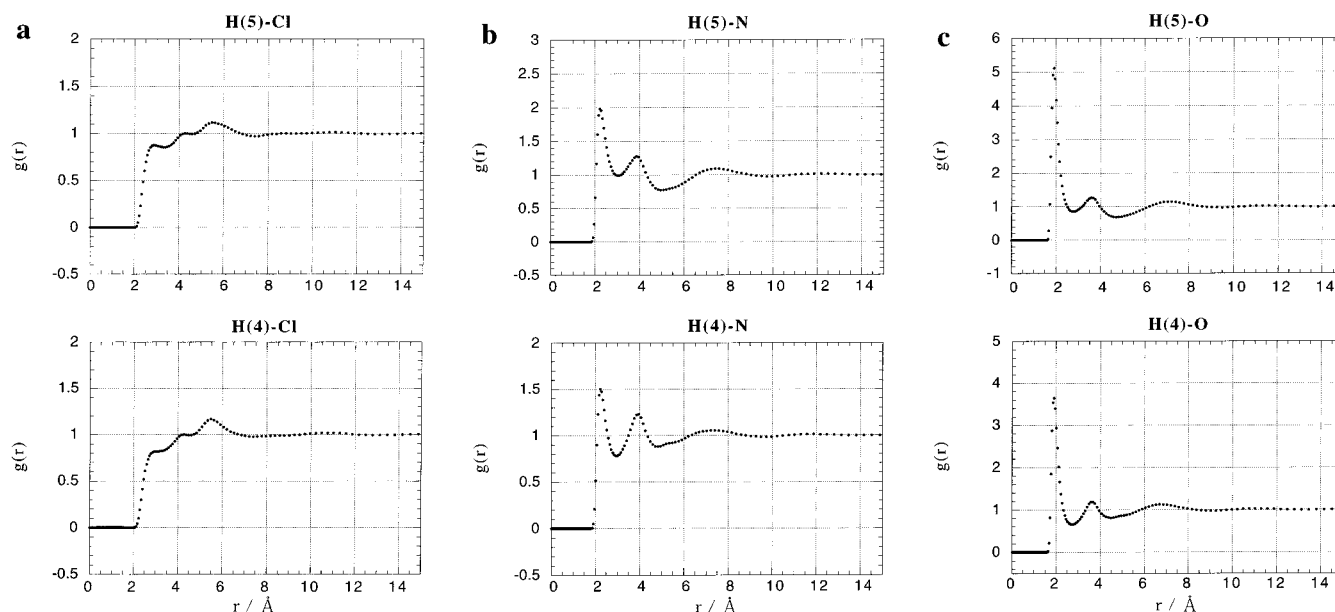


**Figure 3.** Radial distribution functions between the H(4) and H(5) sites of the keto form (formamide) and solvent sites. (a) H–Cl (solvent:  $\text{CCl}_4$ ), (b) H–N (solvent:  $\text{CH}_3\text{CN}$ ), (c) H–O (solvent:  $\text{DMSO}$ ).

**TABLE 2: Partial Charges on Atom Sites in  $\text{CCl}_4$ ,  $\text{CH}_3\text{CN}$ , and  $\text{DMSO}$  (Units in Electronic Charges)**

solvent	keto						enol					
	C	N	O	H(4)	H(5)	H(6)	C	N	O	H(4)	H(5)	H(6)
$\text{CCl}_4$	0.74	-1.06	-0.60	0.47	0.44	0.01	0.58	-0.87	-0.64	0.48	0.38	0.07
$\text{CH}_3\text{CN}$	0.75	-1.04	-0.67	0.48	0.46	0.02	0.63	-0.94	-0.68	0.51	0.41	0.07
$\text{DMSO}$	0.76	-1.07	-0.69	0.49	0.48	0.03	0.66	-1.00	-0.72	0.54	+0.45	0.07

**TABLE 3: Optimized Geometries of Keto–Enol Tautomers in Solutions**

solvent	keto			enol			
	$l(\text{C}=\text{O})^a$	$l(\text{C}-\text{N})^a$	dipole <sup>b</sup>	$l(\text{O}-\text{H}(4))^a$	$l(\text{N}\cdots\text{H}(4))^a$	$\angle\text{OCN}^c$	dipole <sup>b</sup>
$\text{CCl}_4$	1.196	1.353	4.22	0.948	2.312	122.58	1.25
$\text{CS}_2$	1.198	1.351	4.38	0.949	2.321	122.76	1.28
DME	1.204	1.347	4.86	0.952	2.369	123.91	1.37
THF	1.202	1.347	4.73	0.951	2.353	123.50	1.26
$\text{CH}_3\text{CN}$	1.206	1.343	4.99	0.952	2.351	123.23	1.43
$\text{DMSO}$	1.208	1.340	5.21	0.951	2.358	123.28	1.51
gas	1.196	1.353	4.23	0.948	2.309	122.54	1.23

<sup>a</sup> In angstroms. <sup>b</sup> In debyes. <sup>c</sup> In degrees.

**TABLE 4: Total Free Energy Differences, Solvation Free Energies, and Reorganization Energies**

solvent	$\Delta G(\text{keto}-\text{enol})^{a,b}$	$\Delta F_{\text{HNC}}(\text{keto})^b$	$\Delta F_{\text{HNC}}(\text{enol})^b$	$\Delta E_{\text{re}}(\text{keto})^b$	$\Delta E_{\text{re}}(\text{enol})^b$	$\epsilon^c$
$\text{CCl}_4$	-12.60	2.39	2.33	0.00033	0.0012	2.237
$\text{CS}_2$	-12.77	0.51	0.64	0.054	0.040	2.643
DME	-13.37	-4.95	-4.19	0.74	0.69	5.02
THF	-14.41	-5.57	-3.72	0.39	0.28	7.58
$\text{CH}_3\text{CN}$	-14.57	-2.51	-0.084	0.97	0.45	35.94
$\text{DMSO}$	-13.35	-7.78	-6.81	1.70	1.41	46.45
gas	-12.66					

<sup>a</sup>  $\Delta G$  is the difference of eq 4 between the keto and enol form. <sup>b</sup> In kcal/mol. <sup>c</sup> Dielectric constant for each solvent. Data from ref 36.

those of the solute H(4) and H(5) sites. Although the solvation energy at the solute nitrogen site is positive, the negative values for the remaining sites make the total solvation energy negative. Similar results were obtained for the enol tautomer. These indicate that the characteristics of the solvent effect are dominated by the hydrogen bonding.

(c) *Characterization of the Solvent Effect by the Hydrogen Bond.* The empirical solvent parameters derived by Taft and co-workers<sup>2</sup> are well-known as a measure of hydrogen-bonding abilities of solvents. For various kinds of solvents, they determined the parameters for the ability of solvents to donate or accept a proton in solute–solvent hydrogen bonding, the  $\alpha$

**TABLE 5: Contributions of Solute (Keto) Atom to the Solvation Free Energies in  $\text{CCl}_4$ ,  $\text{CH}_3\text{CN}$ , and  $\text{DMSO}$  (Units in kcal/mol)**

solvent	solute site					
	C	N	O	H(4)	H(5)	H(6)
$\text{CCl}_4$	1.00	-0.60	-0.47	0.86	0.97	0.63
$\text{CH}_3\text{CN}$	-1.64	11.34	-1.81	-4.38	-6.50	0.49
$\text{DMSO}$	-4.51	16.17	-2.37	-7.26	-10.24	0.42

parameter (for donating) and  $\beta$  parameter (for accepting). Since we treat aprotic solvents here, it is appropriate to take the  $\beta$  parameter. The values of the  $\beta$  parameter are reported to be

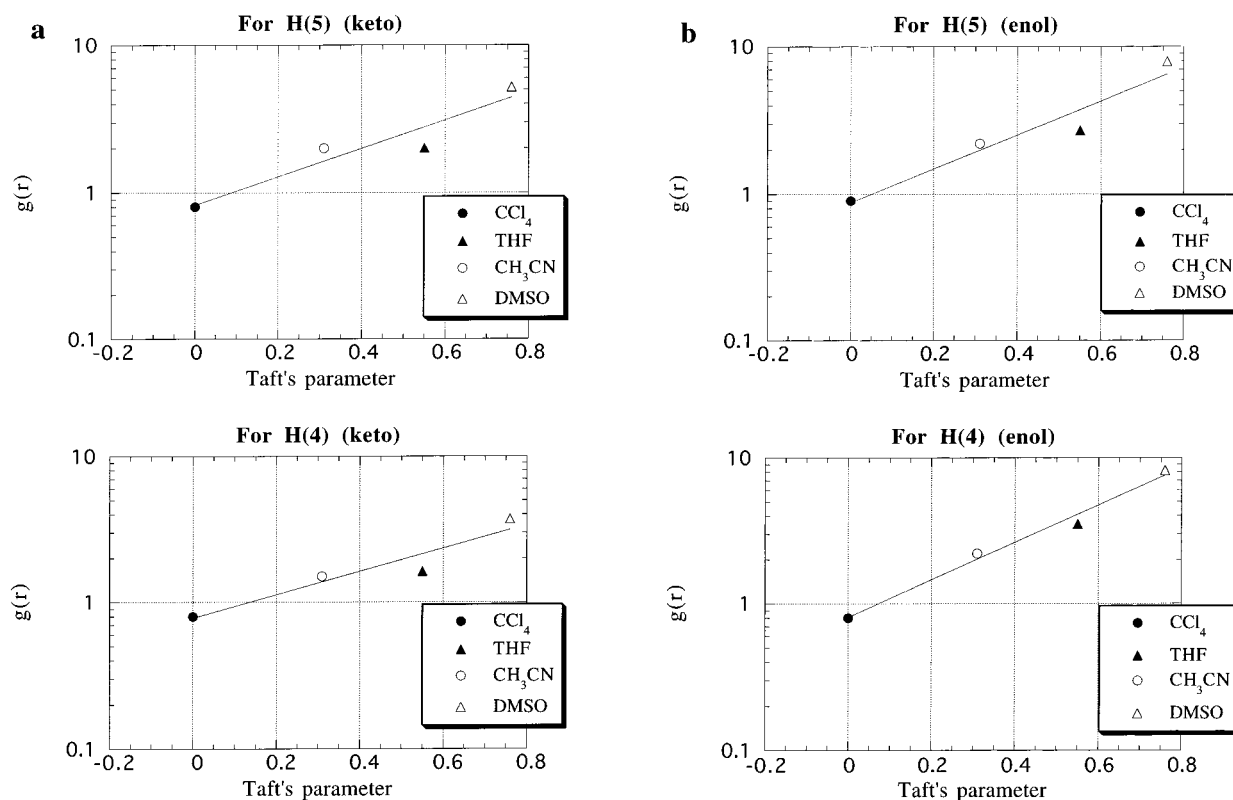


**Figure 4.** Plots of the logarithms of the heights of the first peaks in the rdf's against Taft's  $\beta$  parameters. The abscissa is a logarithmic scale. (a) For the keto form, the positions of the first peaks are 2.8, 2.2, 2.3, and 2.0 Å for  $\text{CCl}_4$ , THF,  $\text{CH}_3\text{CN}$ , and DMSO (for both H(4) and H(5)). (b) For the enol form, the positions of the first peaks are 2.9, 2.0, 2.2, and 1.8 Å for  $\text{CCl}_4$ , THF,  $\text{CH}_3\text{CN}$ , and DMSO (for both H(4) and H(5)).

0.31, 0.55, and 0.76 for acetonitrile, THF, and DMSO, respectively,<sup>2</sup> indicating that the strength of hydrogen bonding in THF or DMSO solutions is larger than in acetonitrile. The  $\beta$  parameter for  $\text{CCl}_4$  is zero. As seen in Figure 3b,c, the height of the first peak is smaller for the acetonitrile solution than that for the DMSO solution. This suggests that the hydrogen-bonding ability of acetonitrile is weaker than that of DMSO. Considering that the solute–solvent hydrogen bonding is represented by the first peak of rdf's and the peak height is related to the well-depth of the mean potential, it would be appropriate to take the logarithm of the height of the first peak as a measure of the strength of hydrogen bonding. In Figure 4, we plotted the heights of the first peaks in a logarithmic scale against Taft's,  $\beta$  parameters for  $\text{CCl}_4$ , THF, acetonitrile, and DMSO solutions. As easily seen, linear correlation is obtained for both the keto and enol tautomers. This indicates that the Taft's parameters are in fact good measures of hydrogen bonding. It is not surprising that the solvation free energy in the acetonitrile solution shows a remarkable irregularity. With these relations, we could qualitatively explain the origin of empirical solvent parameters representing the ability of the solvent to form hydrogen bonding at a molecular level. It is noted that the solvent geometric structures as well as the partial charges on the sites play an important role in determining the solvent parameters.

As seen in Table 3, the calculated solute dipole moments in polar aprotic solvents are larger than that in the gas phase, while those in nonpolar aprotic solvents are not different from the gas-phase value. It is observed that the dipole moment of the keto form is much enhanced from the enol form in polar aprotic solvents. The calculated solute dipole moments, in both of the tautomers, increase as solvent polarities increase. These tendencies show good correlation with the empirical solvent dipolarity/polarizability parameters, the  $\pi^*$  parameter by Taft et al. They

are 0.28, 0.58, 0.75, and 1.00 for  $\text{CCl}_4$ , THF,  $\text{CH}_3\text{CN}$ , and DMSO, respectively.<sup>2</sup> Therefore it is indicated that the enhancement of the solute dipole moment is related to bulk properties of solvents and our calculations also reproduce qualitatively the tendency of the  $\pi^*$  parameter.

#### IV. Conclusion

By using the RISM-SCF method, the optimized geometries and solvation free energies of the keto and enol tautomers of formamide were calculated in six organic aprotic solvents ( $\text{CS}_2$ ,  $\text{CCl}_4$ , DME, THF, acetonitrile, and DMSO). From the analysis of the solvation free energies, it is shown that the solute–solvent hydrogen bonding largely contributes to them and that the ability of the solvent to form hydrogen bonding is very important. It is also shown that Taft's  $\beta$  parameters are well-correlated to the calculated well-depth of the hydrogen bonding. The results that the solvation free energies for both of the tautomers show irregularity in the acetonitrile solution are in qualitative accord with the empirically determined solvent parameters. The empirical measure of the solvent ability to form hydrogen bonding with solute is explained at a molecular level.

The solvent effects on the energy difference between the keto–enol tautomers were examined. It is found that the keto tautomer is stabilized largely compared to the enol form. These tendencies are consistent with the experimental and previous theoretical results. In both tautomers, the dipole moments of solutes are enhanced in polar solvents and the geometric structures are changed, so as to increase the solute dipole moment. It is found that the tendency of solute dipole moments is correlated to Taft's parameters with respect to the solvent polarity.

**Acknowledgment.** We are grateful to Mr. K. Naka for his coding of the grid point generation based on the Voronoi

polyhedrons and Professor N. Hirota for valuable discussions in preparing the manuscript. We also thank Professor W. L. Jorgensen for sending the data of simulation of THF to us and Dr. A. Luzar for the data of simulation of DMSO. This work was supported by the Grant in Aid for Scientific Research from the Ministry of Education.

## References and Notes

- (1) Reichardt, C. *Solvents and Solvent Effects in Organic Chemistry*, 2nd ed.; VCH Verlagsgesellschaft: Weinheim, 1988.
- (2) Kamlet, M. J.; Abboud, J.-L. M.; Abraham, M. H.; Taft, R. W. *J. Org. Chem.* **1983**, *48*, 2877–2887.
- (3) Cramer, C. J.; Truhlar, D. G. In *Solvent Effects and Chemical Reactivity*; Tapia, O., Bertran, J., Eds.; Kluwer: Dordrecht, 1996 and references cited therein.
- (4) Tomasi, J.; Persico, M. *Chem. Rev.* **1994**, *94*, 2027–2094.
- (5) Chandler, D.; Andersen, H. C. *J. Chem. Phys.* **1972**, *57*, 1930–1937.
- (6) Hirata, F.; Rossky, P. J. *J. Chem. Phys. Lett.* **1981**, *83*, 329–334.
- (7) Hirata, F.; Pettitt, B. M.; Rossky, P. J. *J. Chem. Phys.* **1982**, *77*, 509–520.
- (8) Hirata, F.; Rossky, P. J.; Pettitt, B. M. *J. Chem. Phys.* **1983**, *78*, 4133–4144.
- (9) Ten-no, S.; Hirata, F.; Kato, S. *Chem. Phys. Lett.* **1993**, *214*, 391–396.
- (10) Ten-no, S.; Hirata, F.; Kato, S. *J. Chem. Phys.* **1994**, *100*, 7443–7453.
- (11) Sato, H.; Hirata, F.; Kato, S. *J. Chem. Phys.* **1996**, *105*, 1546–1551.
- (12) Kawata, M.; Ten-no, S.; Kato, S.; Hirata, F. *Chem. Phys. Lett.* **1995**, *240*, 199–204.
- (13) Kawata, M.; Ten-no, S.; Kato, S.; Hirata, F. *J. Am. Chem. Soc.* **1995**, *117*, 1638–1640.
- (14) Kawata, M.; Ten-no, S.; Kato, S.; Hirata, F. *J. Phys. Chem.* **1996**, *100*, 1111–1117.
- (15) Kol'tsov, A. I.; Kheifets, G. M. *Russ. Chem. Revs.* **1971**, *40*, 773–788.
- (16) Kol'tsov, A. I.; Kheifets, G. M. *Russ. Chem. Revs.* **1972**, *41*, 452–467.
- (17) Beak, P.; Fry, F. S., Jr.; Lee, J.; Steele, F. *J. Am. Chem. Soc.* **1976**, *98*, 171–179.
- (18) Beak, P. *Acc. Chem. Res.* **1977**, *10*, 186–192.
- (19) Beak, P.; Covington, J. B.; White, J. M. *J. Org. Chem.* **1980**, *45*, 1347–1353.
- (20) Emsley, J. *Struct. Bonding* **1984**, *57*, 147–191.
- (21) Wong, M. W.; Wiberg, K. B.; Frisch, M. J. *J. Am. Chem. Soc.* **1992**, *114*, 1645–1652.
- (22) Sato, H.; Kato, S. *J. Mol. Struct. (THEOCHEM)* **1994**, *310*, 67–75.
- (23) Lowden, L. J.; Chandler, D. *J. Chem. Phys.* **1974**, *61*, 5228–5241.
- (24) Chang, T.-M.; Peterson, K. A.; Dang, L. X. *J. Chem. Phys.* **1995**, *103*, 7502–7513.
- (25) Zhu, S.-B.; Lee, J.; Robinson, G. W. *Mol. Phys.* **1988**, *65*, 65–75.
- (26) Jorgensen, W. L.; Ibrahim, M. *J. Am. Chem. Soc.* **1981**, *103*, 3976–3985.
- (27) Briggs, J. M.; Matsui, T.; Jorgensen, W. L. *J. Comput. Chem.* **1990**, *11*, 958–971.
- (28) Jorgensen, W. L.; Briggs, J. M. *Mol. Phys.* **1988**, *63*, 547–558.
- (29) Luzar, A.; Soper, A. K.; Chandler, D. *J. Chem. Phys.* **1993**, *99*, 6836–6847.
- (30) Jorgensen, W. L.; Swenson, C. J. *J. Am. Chem. Soc.* **1985**, *107*, 569–578.
- (31) Weiner, S. J.; Kollman, P. A.; Case, D. A.; Singh, U. C.; Ghio, C.; Alagona, G.; Profeta, S., Jr.; Weiner, P. *J. Am. Chem. Soc.* **1984**, *106*, 765–784.
- (32) Friesner, R. A. *J. Phys. Chem.* **1988**, *92*, 3091–3096.
- (33) Dunning, T. H., Jr.; Hay, P. J. In *Modern Electronic Structure Theory*; Schaefer, H. F., III., Ed.; Plenum: New York, 1977.
- (34) Singer, S. J.; Chandler, D. *Mol. Phys.* **1985**, *55*, 621–625.
- (35) Zichi, D. A.; Rossky, P. J. *J. Chem. Phys.* **1986**, *84*, 1712–1723.
- (36) Riddick, J. A.; Bunger, W. B.; Sakano, T. K. *Organic Solvents*, 4th ed.; Wiley-Interscience: New York, 1986.
- (37) Böttcher, C. J. F. *Theory of Electric Polarization vol.1*; Elsevier: Amsterdam, 1973; pp 129–157.
- (38) Chandler, D.; Singh, Y.; Richardson, D. M. *J. Chem. Phys.* **1984**, *81*, 1975–1982.